Enhanced Bandwidth Compact Hybrid Rat-Race Coupler for 5G Dual Band Applications

IULIA ANDREEA MOCANU
Department of Telecommunications,
National University of Science and Technology Politehnica Bucharest,
Splaiul Independentei nr. 313, Bucharest,
ROMANIA

Abstract: - A compact hybrid rat-race coupler with dual-band behavior at 2.4 GHz, respectively at 5.2 GHz is presented. The transmission lines used for the design consist of three impedance inverter symmetrical unit cells with complementary behavior. The implementation with real lumped elements shows a very good agreement between the ideal case and the real one. The simulations for the real implementation of the return and isolation losses are around 40 dB, while the insertion and coupling losses are around 3.5 dB at both frequencies. The phase difference at the output ports shows an imbalance of ±1° from the ideal case.

Key-Words: - Rat-race coupler, hybrid coupler, impedance inverter unit cells, dual-band, differential coupler, artificial transmission lines, 5G communications.

Received: May 21, 2024. Revised: October 23, 2024. Accepted: November 19, 2024. Published: December 31, 2024.

1 Introduction

Hybrid rat-race couplers are very common in the microwave domain. They are used to divide power and ensure a phase difference of ±180o between the output signals. Their main drawbacks are the fact they work for only one frequency, and they have a relatively narrow bandwidth, [1], [2].

On the other hand, nowadays the trend in telecommunications is to use multi-band devices with improved performances and reduced dimensions, [3], [4]. To achieve these goals with microwave circuits, new types of materials are introduced. It is the case of metamaterial transmission lines, also known as Left-Handed transmission lines (LH TLs) which are created by chaining a certain number of unit cells with a length much smaller than a quarter of the wavelength, [5].

There are several types of such lines, but the ones that are mostly used in applications are the Composite Right Left-Handed (CRLH) [6] and Dual Composite Right Left-Handed (D-CRLH) [7]. As the names suggest they exhibit both Right Handed and Left Handed properties which allows them to be used for dual-band devices: branch line couplers [8], [9], rat race couplers [10], [11], power dividers [12], [13], diplexers [14], [15] in various technologies: microstrip, stripline, coplanar, lumped [16], [17], [18], [19]. Also, they have dual behavior: the CRLH lines show a bandpass characteristic, while the D-CRLH lines show a stopband one [20], [21]. When designing such transmission lines, it is very important to consider if the working frequencies are in the bandwidth which assures propagation, otherwise, the number of cells must be increased [2], [7]. Sometimes this is not a viable solution because both the losses and dimensions will increase as well.

To overcome these drawbacks, we present in this paper miniaturized CRLH and D-CRLH transmission lines designed to work for two arbitrary frequencies as impedance inverters and have enhanced bandwidth.

2 Dual Band Artificial Transmission Lines

It is known that the conventional rat-race coupler consists of three identical λ/4 transmission lines and one 3λ/4 line, where λ is the wavelength corresponding to a frequency imposed by the application. It means that the first type of line introduces a 90-phase difference, while the second type introduces a 270°/-90° phase difference at the imposed frequency. As shown, the classical transmission lines are single-band components, and consequently, the coupler which is designed with these lines is a single-band component as well.

In this paper, we aim to transform the classical single-band component into a dual-band one, by replacing the classical transmission lines with dual-band ones, such as Composite Right Left-Handed

(CRLH) and Dual Composite Right Left-Handed (D-CRLH). In this paper the first transmission line is replaced by a new dual-band D-CRLH TL which introduces a phase shift of ±90° for two arbitrary frequencies and the second line is replaced by a new dual-band CRLH TL which introduces a phase shift of ∓90° at the two working frequencies.

Each artificial transmission line consists of an odd number of unit cells and each unit cell introduces a phase shift of ±90°/∓90°.

The CRLH unit cell consists of an inductor, with inductance L_R in series with a capacitor, of capacitance C_L, placed in the longitudinal branch, respectively of an inductor, with inductance L_L in parallel with a capacitor of capacitance C_R, placed in the transversal branch.

The D-CRLH unit cell, consists of other lumped components placed in a dual configuration: a parallel connection between L_R and C_L in the longitudinal branch and a series connection between L_L and C_R in the transversal branch. The constitutive parameters given by L_R, C_R, L_L and C_L depend on the two arbitrary frequencies, ω_1, ω_2 and the characteristic impedance, Z_C. The computational relations for one CRLH unit cell are [22]:

$$L_R = \frac{1}{k-1}\cdot\frac{Z_c}{\omega_1}; \tag{1}$$

$$C_L = \frac{k-1}{k}\cdot\frac{1}{\omega_1\cdot Z_c}; \tag{2}$$

$$C_R = \frac{1}{k-1}\cdot\frac{1}{\omega_1.Z_c}; \tag{3}$$

$$L_L = \frac{k-1}{k}\cdot\frac{Z_c}{\omega_1}; \tag{4}$$

respectively for one D-CRLH unit cell, [23]:

$$L_L = \frac{1}{k-1}\cdot\frac{Z_c}{\omega_1}; \tag{5}$$

$$C_R = \frac{k-1}{k}\cdot\frac{1}{\omega_1\cdot Z_c}; \tag{6}$$

$$C_L = \frac{1}{k-1}\cdot\frac{1}{\omega_1.Z_c}; \tag{7}$$

$$L_R = \frac{k-1}{k}\cdot\frac{Z_c}{\omega_1}; \tag{8}$$

where Z_c is the characteristic impedance of the transmission line and $k = \omega_2/\omega_1$ represents the ratio between the two angular working frequencies.

If we want the power to be divided equally by the rat-race coupler, then the characteristic impedance for all transmission lines is set to Z_C=70.71 Ω. Also, the microwave frequencies are chosen from 5G standards: f_1=2.4 GHz, respectively f_2=5.2 GHz. In these conditions we compute using relations (1)-(4) and (5)-(8) the values for the constitutive lumped elements of one CRLH unit cell: L_R=4.0192 nH, C_L=0.5049 pF, L_L=2.5249 nH, C_R=0.8038 pF., respectively for one D-CRLH unit cell: L_L=4.0192 nH, C_R=0.5049 pF, L_R=2.5249 nH, C_L=0.8038 pF.

As we want to increase the bandwidth of the artificial transmission line, three-unit cells instead of one will be chosen for the design.

The scheme of the ideal CRLH transmission line is presented in Figure 1 and its performances obtained after simulation with Ansoft Designer SV are given in Figure 2 and Figure 3. Markers are placed in both figures at the imposed frequencies to measure the values of the simulated parameters.

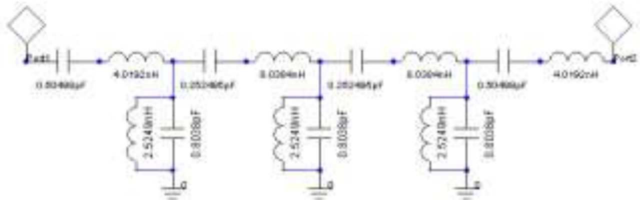

Fig. 1: The ideal inverter CRLH transmission line with three cells

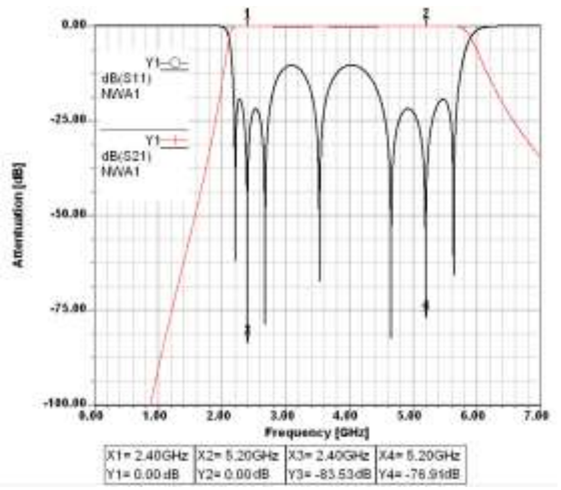

Fig. 2: Return loss, S_{11}, and insertion loss, S_{21} for the ideal inverter CRLH transmission line with three cells

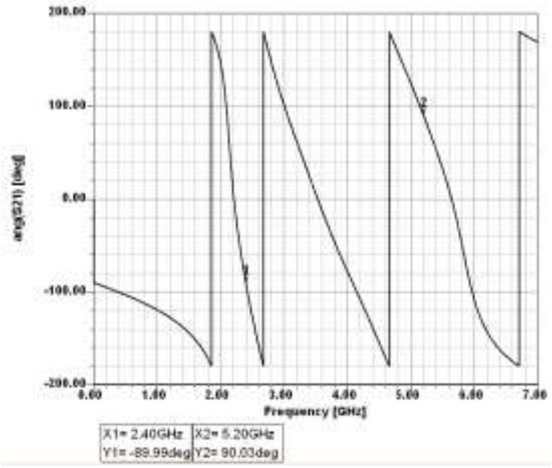

Fig. 3: Phase difference for the ideal inverter CRLH transmission line with three cells

Figure 2 shows that port 1 is perfectly matched (there are no reflections at port 1 and the whole power at port 1 is transferred to port 2, the output port), so the return loss is very high, ideally infinite at the two imposed frequencies: -83.53 dB, respectively -76.91 dB. Also, in Figure 2 we observe that the insertion loss is 0 dB, at both imposed frequencies, showing we have full transfer from the input port to the output port, as in the theoretical model.

Nevertheless, Figure 3 shows that the phase difference is -89.99° for the first frequency, respectively 90.03° for the second frequency in comparison to -90°, respectively 90° in the theoretical case.

Next, a comparison between the results obtained for a CRLH transmission line with one unit cell, three-unit cells and five-unit cells is carried. The algorithm to design the lines in all three cases is similar to the one presented previously. Based on the simulations in the ideal case and imposing a variation of the insertion loss of 0.2 dB in the ideal case, the values for the bandwidth are given in Table 1.

Table 1. The bandwidth-BW for the ideal CRLH transmission lines with one-unit cell, three-unit cells, and five-unit cells

Operating central frequency	**f_1=2.4 GHz**	**f_2=5.2 GHz**
One unit cell TL BW [GHz]	0.51	1.12
Three-unit cells TL BW [GHz]	0.76	1.41
Five-unit cells TL BW [GHz]	0.5	1.02

So, the results from Table 1 show that the largest bandwidth is obtained for three unit-cells transmission line, and this one will be implemented using real components.

For the lumped elements, Surface Mounted Devices (SMDs) are chosen to have a high-quality factor at high frequencies and low parasitic elements. The selected packages are chip, 0603 type, with the following dimensions: length-1.55±0.05 mm, width-0.85±0.05 mm, height-0.45±0.05 mm (60 x 30 x 20 mil, in Imperial System). The small-size chip passive components help to minimize the overall circuit. The lumped elements used to implement the coupler are AVX Accu-L 0603 for inductors with a quality factor of around 60 and tight tolerances of ±0.1 nH, respectively AVX UQCS for capacitors, having a quality factor of around 250. Another aspect to be considered in the design is the fact that the standardized values are far from the computed ones, so, series and parallel groups are needed to achieve overall values as close as possible to the computed ones. The combinations for the CRLH transmission line are given in Table 2.

The markers placed at the two working frequencies to measure the values of the transmission parameters show that the implemented CRLH transmission line can be used to create the coupler.

Table 2. Real components for the implementation of the CRLH transmission lines

Lumped elements	**Ideal case**	**Available components**
$L_R/2$ [nH]	4.0192	1.8 nH in series with 2.2 nH =4 nH
L_R [nH]	8.0384	3.3 nH in series with 4.7 nH=8 nH
L_L [nH]	2.5249	2.7 nH in parallel with 2.7 nH in series with 1.2 nH =2.55 nH
$2C_L$ [pF]	0.50499	0.5 pF
C_L [pF]	0.252495	0.2 pF in parallel with 0.1 pF in series with 0.1 pF =0.25 pF
C_R [pF]	0.8038	0.8 pF

After implementation, a simulation of the performances is run with Ansoft Designer SV and the results are given in Figure 4 and Figure 5.

When using real components, there can be noticed the influence of the losses, especially for the values of the insertion loss which is now -0.39 dB, respectively -0.34 dB at the two frequencies instead of the 0 dB in the ideal case. Also, because of the losses and approximations, the return loss is -38.28 dB, respectively -45.39 dB for the two frequencies and not -83.53 dB, respectively -76.91 dB as in the ideal case. The phase difference remains very close to the ideal $\mp 90^{o}$ being -89.77^{o}, respectively 92.38^{o}, thus allowing us to use this type of transmission line for our further design.

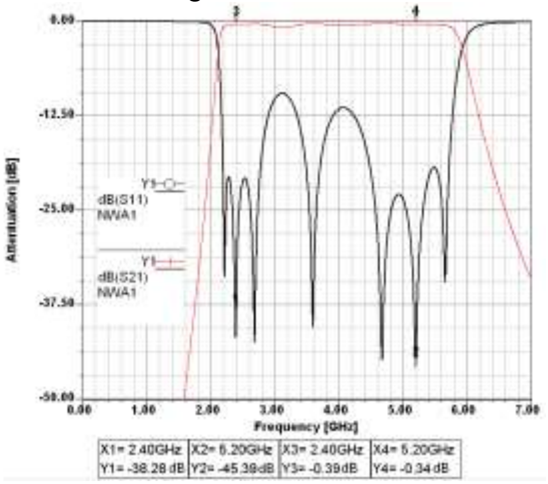

Fig. 4: Return loss, $S_{11,}$ and insertion loss, S_{21} for the implemented inverter CRLH transmission line with three cells

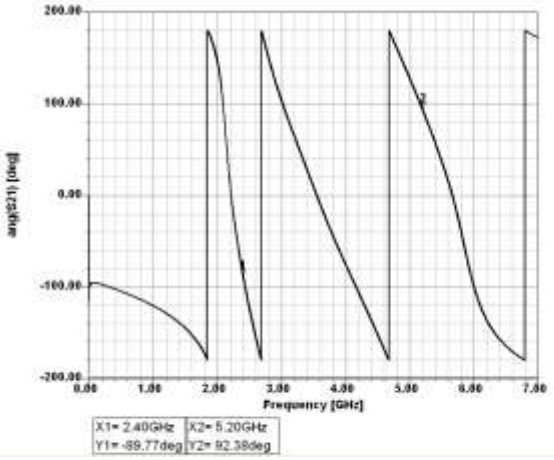

Fig. 5: Phase difference for the implemented inverter CRLH transmission line with three cells

The second type of transmission line is the D-CRLH one made of three identical unit cells, as presented in Figure 6. The results after simulation with Ansoft Designer SV for the ideal case are given in Figure 7 and Figure 8.

In Figure 7 one can see the stop-band behavior of the D-CRLH transmission line, different from the pass-band behavior of the CRLH transmission line (Figure 2).

Figure 7 shows that port 1 is perfectly matched (there are no reflections at port 1 and the whole power at port 1 is transferred to port 2, the output port), so the return loss is very high, ideally infinite at the two imposed frequencies: -103.89 dB, respectively -96.99 dB. Also, in Figure 7 we observe that the insertion loss is 0 dB, at both imposed frequencies, showing we have full transfer from the input port to the output port, as in the theoretical model. Nevertheless, Figure 8 shows that the phase difference is 90.01^{o} for the first frequency, respectively -89.97^{o} for the second frequency in comparison to 90^{o}, respectively -90^{o} in the theoretical case.

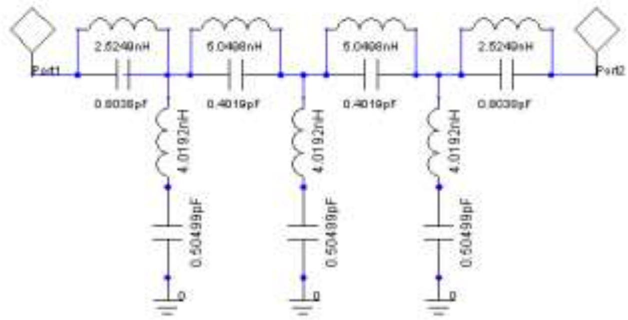

Fig. 6: The ideal inverter D-CRLH transmission line with three cells

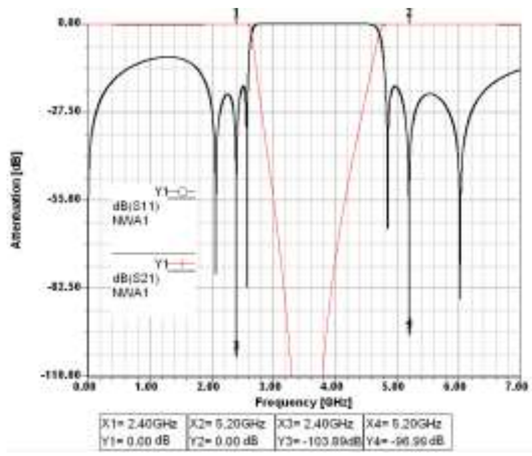

Fig. 7: Return loss, $S_{11,}$ and insertion loss, S_{21} for the ideal inverter D-CRLH transmission line with three cells

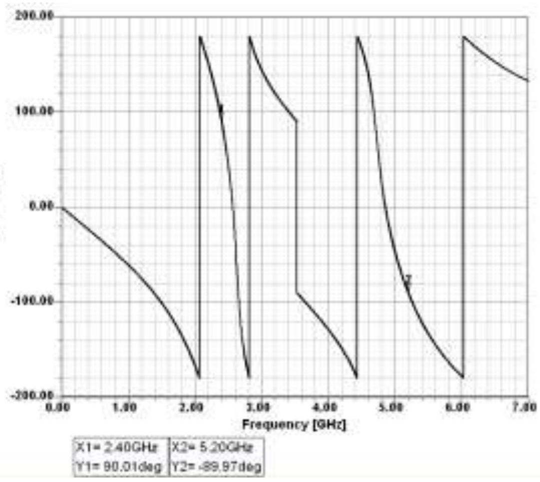

Fig. 8: Phase difference for the ideal inverter D-CRLH transmission line with three cells

Next, a comparison between the results obtained for a D-CRLH transmission line with one unit cell, three-unit cells and five-unit cells is done. The algorithm to design the lines in all three cases is like the one presented previously. Based on the simulations in the ideal case and imposing a variation of the insertion loss of 0.2 dB in the ideal case, the values for the bandwidth are given in Table 3.

Table 3. The bandwidth-BW for the ideal D-CRLH transmission lines with one-unit cell, three-unit cells, and five-unit cells

Operating central frequency	**f_1=2.4 GHz**	**f_2=5.2 GHz**
One unit cell TL BW [GHz]	0.53	1.34
Three-unit cells TL BW [GHz]	0.8	2.14
Five-unit cells TL BW [GHz]	0.97	2.3

So, the results from Table 3 show that the largest bandwidth is obtained for three unit-cells transmission line, and this one will be implemented using real components.

Also, if we compare the bandwidths for three-cells CRLH and D-CRLH TLs, we can observe that the largest bandwidth is obtained for D-CRLH line and this justifies using it to replace three classical lines rather than just one.

In Figure 8, by analyzing the values of the phase difference at the two working frequencies given by the two markers, one can see the dual behavior of the D-CRLH line in comparison with the behavior of the CRLH one. Again, we have a great agreement between simulation and theory.

The next step, as in the case of the CRLH transmission line, is to implement the line with real available components. We also use AVX Accu-L 0603 for inductors and AVX UQCS for capacitors with the same characteristics explained in the case of the CRLH TL implementation. The series and parallel combinations of components for the D-CRLH transmission line are given in Table 4.

The results of the simulation with Ansoft Designer SV are the ones in Figure 9 and Figure 10.

In Figure 9 there are placed markers at the two working frequencies to measure the return loss and insertion loss, meanwhile in Figure 10, the markers are placed at the two frequencies to measure the phase difference introduced by the real D-CRLH transmission line.

Table 4. Real components for the implementation of the D-CRLH transmission lines

Lumped elements	**Ideal case**	**Available components**
$L_R/2$ [nH]	2.5249	2.7 nH in parallel with 2.7nH in series with 1.2 nH=2.55 nH
L_R [nH]	5.0498	10 nH in parallel with 10 nH=5 nH
L_L [nH]	4.0192	1.8 nH in series with 2.2 nH =4 nH
$2C_L$ [pF]	0.8038	0.8 pF
C_L [pF]	0.4019	0.4 pF
C_R [pF]	0.50499	0.5 pF

When using real components, there can be noticed the influence of the losses, especially for the values of the insertion loss which is now -0.37 dB, respectively -0.35 dB at the two frequencies instead of the 0 dB in the ideal case. Also, because of the losses and approximations, the return loss is -31.87 dB, respectively -35.31 dB for the two frequencies and not -103.89 dB, respectively -96.99 dB as in the ideal case.

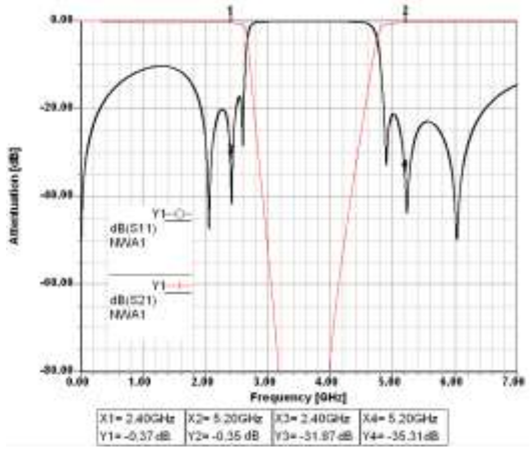

Fig. 9: Return loss, S_{11}, and insertion loss, S_{21} for the implemented inverter D-CRLH transmission line with three cells

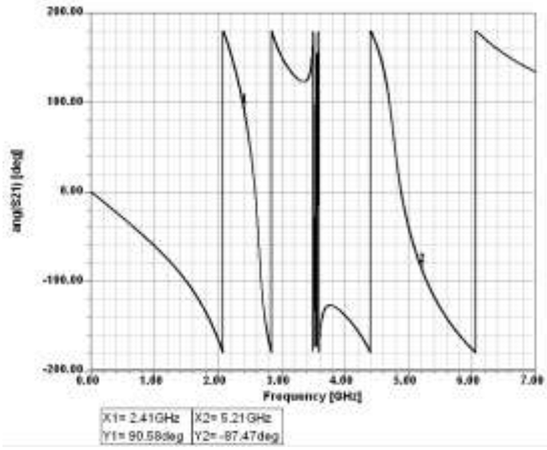

Fig. 10: Phase difference for the implemented inverter D-CRLH transmission line with three cells

The phase difference remains very close to the ideal ±90° being 90.58°, respectively -87.47°, thus allowing us to use this type of transmission line for our further design.

The results obtained for the CRLH and D-CRLH transmission lines implemented with real components with a finite quality factor show that the losses appear and affect both the return loss and the insertion loss, but still the performances are as expected.

3 Dual Band Differential Hybrid Coupler

The differential hybrid coupler is implemented as suggested previously in Chapter 2 with CRLH and D-CRLH inverter transmission lines. As shown in Figure 3 and Figure 8, the CRLH line introduces -89.99° at 2.4GHz, respectively 90.03° at 5.2GHz, so it acts as a 3λ/4 classical line but at two arbitrary frequencies, while the D-CRLH line introduces 90.01° at 2.4GHz, respectively -89.97° at 5.2GHz, so it acts as a λ/4 classical line but at two arbitrary frequencies. These observations remain valid for the real-case implementation of the transmission lines.

In order to make a comparison between the ideal and real coupler, we have created the real coupler with port 1 as the input port, port 2 as the transmission port, port 3 as the isolated port, and port 4 as the coupled port and the ideal coupler for which port 5 is the input port, port 6 is the transmission port, port 7 is the isolated port and port 8 is the coupled port. In Figure 11 there are given the results of the return loss for the real and ideal coupler, S_{11} and $S_{55,}$ and of the isolation loss for the real and ideal coupler, S_{31} and S_{75}.

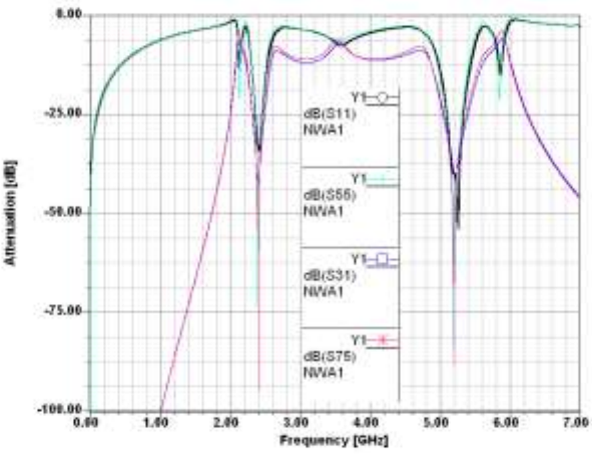

Fig. 11: Return loss, for the real and ideal coupler, S_{11} and S_{55}, respectively the isolation loss for the real and ideal coupler S_{31}, respectively, S_{75}

It can be seen that the ideal and real case exhibit similar characteristics, the only difference is the values of the parameters at the two working frequencies. In the real case, the values for the return loss are 32.21 dB , respectively 39.76 dB in comparison to 88.03 dB , respectively 85.2 dB. For the isolation loss, in the real case there have been measured 41.42 dB, respectively 40.65 dB in comparison to 94.77 dB, respectively 88.13 dB in the ideal case. These values are smaller than in the ideal case, because of the losses modeled by the finite quality factor considered for the lumped components. Also, the approximations done when the implementation with real components was carried out led to some small frequency shifts in the case of the return loss, for the second bandwidth, so that the best value is obtained for 5.25 GHz instead of 5.2 GHz as imposed by design.

In Figure 12 there are given the results for the insertion and coupling loss for the real and ideal coupler case of the coupler (S_{21}, respectively S_{65} and S_{41}, respectively S_{85}).

Based on the data in Figure 12, we can determine for real components that the insertion loss and coupling loss are around 3.5 dB instead of 3 dB as desired in the ideal case. This fact shows that the losses play an important role, so high-quality components are needed to implement the coupler. Otherwise, we notice that the behavior of the coupler even with real components is as expected in the ideal case.

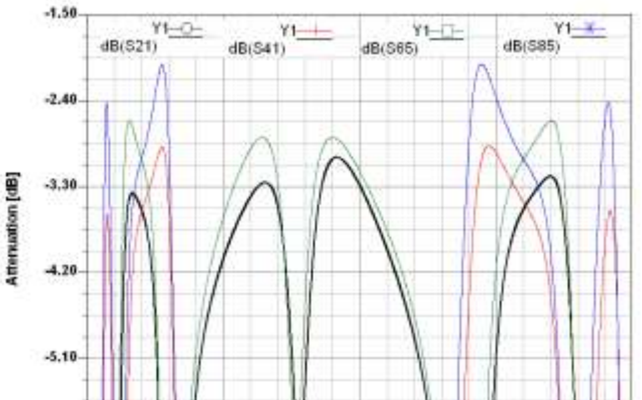

Fig. 12: Insertion loss for the real (S_{21}) and ideal coupler (S_{65}) and coupling loss for the real (S_{41}) and real ideal (S_{85})

In Figure 13, there is depicted the phase difference between the signals at the output ports in the real and ideal coupler case.

DOI: 10.37394/23201.2024.23.28

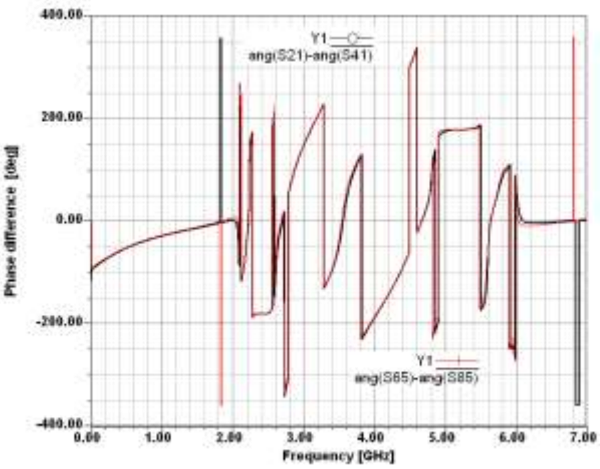

Fig. 13: Phase difference between the signals at the output ports in the real and ideal coupler case implementation of the rat race coupler

For the real case, a phase difference of -181.04°, respectively 178.88° is determined rather than -180°, respectively 180° in the ideal case. This means that the losses do not affect the phase difference between signals at the output ports.

The data discussed previously are synthesized below. For a better comparison between the results obtained in the ideal case and the real one, the main parameters are given in Table 5 at the two imposed frequencies.

Table 5. The main parameters for real and ideal rat race coupler

Operating frequency	**f_1=2.4 GHz**		**f_2=5.2 GHz**	
Type of coupler	Ideal	Real	Ideal	Real
Return loss [dB]	88.03	32.21	85.23	39.76
Isolation loss [dB]	94.77	41.42	88.13	40.65
Insertion loss [dB]	3.01	3.52	3.01	3.46
Coupling loss [dB]	3.01	3.59	3.01	3.52
Phase difference at output ports [°]	-180	-181	180	178.9

The results from Table 5 show great agreement between the ideal and real cases. The coupler's performances are similar at both frequencies and the dual band behavior is demonstrated. As expected, because of the approximations, the phase difference at the output ports shows an imbalance of ±1° from the ideal case.

The effect of the losses can be seen especially for the insertion and coupling losses, so high-quality components are needed when designing the coupler.

To evaluate the relative bandwidth, we impose in the real case for the return and isolation losses to be greater than 15 dB, BW_{15dB}, and for the insertion and coupling losses to have an imbalance of ±1.5 dB.

By imposing the threshold of 15 dB for the return loss, we determine a frequency range between 2.58 GHz and 2.22 GHz, respectively between 5.51 GHz and 4.89 GHz, which means a relative bandwidth of 15%, respectively 12% for both central frequencies. Imposing the same threshold for the isolation loss, we determine a frequency range between 2.6 GHz and 2.2 GHz, respectively between 5.6 GHz and 4.7 GHz, which means a relative bandwidth of 16.6%, respectively 17.3% for both central frequencies. For the coupling loss we determine a bandwidth of 0.48 GHz, respectively 1.04 GHz, which corresponds to a relative bandwidth of 20%, while the insertion loss shows a bandwidth of 0.55 GHz, respectively 1.25 GHz, which corresponds to a relative bandwidth of 24%.

In literature, other dual-band rat-race couplers have been reported with different performances. In [12], there is proposed a coupler designed using stepped impedance stub lines, which has a relative bandwidth for the insertion loss of 21% for the 2.4 GHz and 12% for 5.8 GHz, instead of 24% as in this paper for similar frequencies.

The coupler presented in [24] is implemented using differential bridged-T coils and for it there are reported an input return loss of 24.2 dB and an isolation loss of 38.2 dB at 2.45 GHz. At the second frequency, 5.5 GHz, the input return loss is 17.3 dB, whereas the isolation loss is 22.3 dB.

Another rat-race coupler is reported in [25] and is designed using synthetic transmission lines. The relative bandwidth for this coupler, determined by imposing a 10 dB threshold for the isolation loss is 42 % for the 2.45 GHz and 4.27 % for 5.8 GHz.

The coupler proposed in this work has similar performances at both frequencies and they are mostly better than the ones reported in literature.

If we compare the results obtained in this study to the ones from a classical single-band rat-race coupler, implemented in microstrip technology, then imposing the same conditions, we compute a relative bandwidth for the coupler of around 30 %.

Even if the bandwidth is 10 % larger, the main disadvantage is working at only one frequency. Instead, the proposed coupler works for both frequencies with similar performances and slightly smaller bandwidths and improved performances than the reported couplers in literature.

4 Conclusion

In this paper, we present a rat race coupler designed using the novel Composite Right Left-Handed and

Dual Composite Right Left-Handed transmission lines with enhanced bandwidth for dual-band behavior at 2.4 GHz and 5.2 GHz. Their dual behavior in frequency helps minimize the dimensions but provides very good performances at two microwave arbitrary frequencies, 2.4 GHz and 5.2 GHz.

To enhance the bandwidth, we considered for each transmission line three-unit cells that act as inverters. We have determined the bandwidth for one-unit cell, three-unit cells, and five-unit cells CRLH and D-CRLH transmission lines and we concluded that the largest bandwidth with minimum components is obtained for three-unit cells D-CRLH transmission lines. This allows us to implement the coupler in this topology to enhance the overall bandwidth. The implementation is done with SMD lumped components with high quality to reduce the overall losses. Also, series and parallel groups are needed to achieve equivalent values for the lumped elements as close as possible to the computed ones. This ensures very small shifts in frequency.

The newly proposed rat race coupler shows very good agreement between the performances in the ideal case and the real one. The return and coupling losses are around 40 dB, while the insertion losses are around 3.5 dB. Also, the phase imbalance is around $\pm 1^{o}$ for both frequencies. We have obtained a bandwidth of 24% for both frequencies for the isolation loss and 20% for the return loss. These performances are improved when compared to the similar couplers reported in the literature.

References:

[1] C. Y. Pon, Hybrid-ring directional coupler for arbitrary power division, *IRE Trans. Microw. Theory Tech.,* vol. MTT-9, pp.529 -535 1961, doi: 10.1109/TMTT.1961.1125385

[2] C. Caloz, T. Itoh, *Electromagnetic Metamaterials: Transmission Line Theory and Microwave Applications*, John Wiley & Sons, Inc., Hoboken, New Jersey, pp. 215-216, 2006.

[3] A. B. Shallah, F. Zubir, M. K. A. Rahim, N. M. Jizat, A. Basit, M. Assaad, H. A. Majid, A Miniaturized Metamaterial-Based Dual-Band 4×4 Butler Matrix with Enhanced Frequency Ratio for Sub-6 GHz 5G Applications, in *IEEE Access*, vol. 12, pp. 32320-32333, 2024, doi: 10.1109/ACCESS.2024.3371027.

[4] Y. -H. Ji, C. -H. Chen and W. Wu, Miniaturized Ku/Ka Dual-Band Rat-Race Coupler With Dual Transmission Lines, *2023 16th UK-Europe-China Workshop on Millimetre Waves and Terahertz Technologies (UCMMT)*, Guangzhou, China, 2023, pp. 1-3, doi: 10.1109/UCMMT58116.2023.10310486.

[5] C. Caloz, H. Okabe, T. Iwai, and T. Itoh, Transmission line approach of left-handed (LH) materials, *USNC/URSI National Radio Science Meeting*, vol. 1, p. 39, San Antonio, TX, June 2002.

[6] A. Lai, C. Christophe, and T. Itoh, Composite right/left-handed transmission line metamaterials, *IEEE Microwave Magazine*, vol. 5, no. 3, pp. 34-50, September 2004, doi: 10.1109/TAP.2004.827249.

[7] Caloz, C., Dual Composite Right/Left-Handed (D-CRLH) Transmission Line Metamaterial, *Microwave and Wireless Components Letters, IEEE* , vol.16, no.11, pp.585,587, Nov. 2006, doi: 10.1109/LMWC.2006.884773.

[8] I.-H. Lin, C. Caloz, and T. Itoh, A branch line coupler with two arbitrary operating frequencies using left-handed transmission lines, *IEEE MTT-S Int. Microw. Symp. Dig.*, Philadelphia, PA, USA, vol. 1, pp. 325-328, June 2003, doi: 10.1109/MWSYM.2003.1210944.

[9] R. M. Khattab and A. -A. T. Shalaby, Metamaterial-Based Broadband Branch-Line Coupler and its Application in a Balanced Amplifier, *2021 International Conference on Electronic Engineering (ICEEM)*, Menouf, Egypt, 2021, pp. 1-7, doi: 10.1109/ICEEM52022.2021.9480615.

[10] K.-S. Chin, K.-M. Lin, Y.-H. Wei, T.-H. Tseng and Y.-J. Yang, Compact dual-band branch-line and rat-race couplers with stepped-impedance-stub lines, *IEEE Trans. Microw. Theory Tech.*, vol. 58, no. 5, pp.1213-1221, 2010, doi: 10.1109/TMTT.2010.2046064.

[11] Pei-Ling Chi; Tse-Yu Chen, Dual-Band Ring Coupler Based on the Composite Right/Left-Handed Folded Substrate-Integrated Waveguide, *Microwave and Wireless Components Letters, IEEE*, vol.24, no.5, pp.330,332, May 2014, doi: 10.1109/LMWC.2014.2309087.

[12] T. Huang Taotao Huang, Linping Feng, Li Geng, Haiwen Liu, Shao Yong Zheng, Sheng Ye, Lina Zhang, and Hao Xu , Compact Dual-Band Wilkinson Power Divider Design Using Via-Free D-CRLH Resonators for Beidou Navigation Satellite System, in *IEEE Transactions on Circuits and Systems II: Express Briefs*, vol. 69, no. 1, pp. 65-69, Jan. 2022, doi: 10.1109/TCSII.2021.3085093.

[13] Xue Ren; Kaijun Song; Maoyu Fan; Yu Zhu; Bingkun Hu, Compact Dual-Band Gysel Power Divider Based on Composite Right- and Left-Handed Transmission Lines, *Microwave and Wireless Components Letters, IEEE*, On page(s): 82 - 84 Vol. 25, Issue: 2, Feb. 2015, doi: 10.1109/LMWC.2014.2372481.

[14] Mansour, M.M.; Shalaby, A.-A.T.; El-Rabaie, E.-S.M.; Messiha, N.W., Design and simulation of microwave diplexer based on D-CRLH metamaterials, *Engineering and Technology (ICET), 2014 International Conference on Engineering and Technology (ICET), Cairo,* 2014, pp. 1-5, doi: 10.1109/ICEngTechnol.2014.7016782.

[15] H. Y. Zeng , G. M. Wang , D. Z. Wei and Y. W. Wang, Planar diplexer using composite right-.left-handed transmission line under balanced condition, *Electron. Lett*., vol. 48, no. 2, pp.104-106, 2012, doi: 10.1049/el.2011.2763.

[16] Colin, Daniel Decle; Hu, Zhirun, Uniplanar metamaterial based dual composite right-/-left handed (D-CRLH) microstrip line for microwave circuit applications, *Microwave Conference (APMC), 2014 Asia-Pacific*, Sendai, Japan, 2014, pp.211,213, 4-7 Nov. 2014.

[17] Choi, J.H.; Wu, C.-T.M.; Hanseung Lee; Itoh, T., Vialess composite right/left-handed stripline and its applications for broadband 3-dB and tunable couplers, *European Microwave Conference (EuMC)*, 2014, Rome, Italy, 44th , vol., no., pp.315,318, 6-9 Oct. 2014, doi: 10.1109/EuMC.2014.6986433.

[18] Shih-Chia Chiu; Chien-Pai Lai; Shih-Yuan Chen, Compact CRLH CPW Antennas Using Novel Termination Circuits for Dual-Band Operation at Zeroth-Order Series and Shunt Resonances, *IEEE Transactions on Antennas and Propagation*, vol.61, no.3, pp.1071,1080, March 2013, doi: 10.1109/TAP.2012.2227102.

[19] H. -C. Lu, Y. -L. Kuo, P. -S. Huang and Y. -L. Chang, Dual-band CRLH branch-line coupler in LTCC by lump elements with parasite control, *2010 IEEE MTT-S International Microwave Symposium*, Anaheim, CA, USA, 2010, pp. 393-396, doi: 10.1109/MWSYM.2010.5517669.

[20] A. Sanada, C. Caloz, and T. Itoh, Characteristics of the Composite Right/Left-Handed Transmission Lines, *IEEE Microwave and Wireless Components Letter*, Vol. 14, No.2, Feb. 2004, doi: 10.1109/LMWC.2003.822563.

[21] Wang, Y., Yoon, K.-C. and Lee, J.-C. (2014), A compact transmission line with dual-band filter characteristics using a CRLH metamaterial, *Microw. Opt. Technol. Lett*., 56: 2150–2153, doi: 10.1002/mop.28546.

[22] I.A. Mocanu, Gh. Sajin, Dual band branch-line coupler using novel CRLH transmission lines, *Metamaterials '2012: The Sixth International Congress on Advanced Electromagnetic Materials in Microwaves and Optics*, St. Petersburg, Russia, pp. 306-309, September 2012.

[23] I.A. Mocanu and T. Petrescu, Dual band Wilkinson power divider with artificial transmission lines for mobile TV services, *2014 11th International Symposium on Electronics and Telecommunications (ISETC)*, Timisoara, Romania, 2014, pp. 1-4, doi: 10.1109/ISETC.2014.7010746.

[24] Y. -S. Lin, Y. -R. Liu and C. -H. Chan, Novel Miniature Dual-Band Rat-Race Coupler With Arbitrary Power Division Ratios Using Differential Bridged-T Coils, in *IEEE Transactions on Microwave Theory and Techniques*, vol. 69, no. 1, pp. 590-602, Jan. 2021, doi: 10.1109/TMTT.2020.3035287.

[25] Chen, C.-C., Sim, C.Y.D. and Wu, Y..-J., Miniaturised dual-band rat-race coupler with harmonic suppression using synthetic transmission line, *Electron. Lett*., 52: 1784-1786, 2016, doi: 10.1049/el.2016.2154.

Contribution of Individual Authors to the Creation of a Scientific Article (Ghostwriting Policy)
The authors equally contributed in the present research, at all stages from the formulation of the problem to the final findings and solution.

Sources of Funding for Research Presented in a Scientific Article or Scientific Article Itself
This work was supported by a grant from the National Program for Research of the National Association of Technical Universities - GNAC ARUT 2023.

Conflict of Interest
The authors have no conflicts of interest to declare.